33RD CONGRESS
OF THE INTERNATIONAL COUNCIL
OF THE AERONAUTICAL SCIENCES
STOCKHOLM, SWEDEN, 4-9 SEPTEMBER, 2022

ICAS 2022 SWEDEN

ECONOMICS OF SUSTAINABLE REGIONAL AIR MOBILITY

Pablo de Felipe & Dr. Daqing Yang

Department of Aeronautics, Imperial College London, UK

Abstract

The following study presents the methodology of analysing and sizing 4 different architectures of propulsion systems which include parallel and series hybrids, hydrogen fuel cell and finally fully electric retrofits. These are sized using a simplified methodology based on weight and power restriction imposed by the original aircraft. The performance is bench marked on a typical regional mission. Results show that parallel retrofits are able to save up to 20% in fuel while improving operating costs by 16%. On a short mission, the hydrogen retrofit has the greatest improvement in operating costs if grey hydrogen is used.

Keywords: Sustainable Aviation, hybrid electric, hydrogen fuel cell, economics, performance analysis, retrofits

1. Introduction

Sustainable Regional Air Mobility has the potential of disrupting the airline industry with electrification of aircraft. This may bring the 'third revolution' in the aircraft industry. Nevertheless, in order for operators and governments to support this new field, the economic case must be settled. This report aims at quantifying the direct operating costs derived from fuel and electricity costs for the following propulsion architectures: series and parallel electric hybrids, hydrogen fuel cells and fully electric.

The report begins with a literature review in section 2. Next, the methodology is presented in section 3.and is split into two parts: the first covering the design of the propulsion system and the second the mission analysis. Finally in section 4.the sizing and mission analysis methodology is applied to a case study concerning the retrofit of a Piper Navajo and the results of the design and the costs derived from the fuel consumption are presented.

2. Literature Review

Although this paper only focuses on the costs derived from the fuel and electricity consumed from each of the retrofits, the economics encompass a much broader spectrum of fields such as passenger demand, retrofitted propulsion system price and energy production investigations. As such this literature review will try to cover these aspects irrespective of the fact this paper only focuses on the mission performance estimation and derives costs only from this metric.

Regional Air Mobility is having a resurgence in interest from what is being called the 'Third revolution' in aviation by Moore [1] which calls for higher 'On Demand' options while still having a profitable business. The socio-economic setting of regional transport is investigated by Kreimeir et al. [2]. Here the Air Mobility transportation is carried out by a conceptual battery powered CS-23 aircraft design and the economics compared with ground transportation methods. It must be noted that many research papers currently focus on fully electric aircraft which assume improvements in battery energy density [3][4] coupled with improvements due to the electric propulsion system integration. This is well explained by Moore in [5]. Nevertheless it is clear from this that any retrofitted aircraft will struggle to reap the full benefits of electric propulsion, calling for a clean sheet design.

Hybrid aircraft design and analysis methods have been extensively researched in [6][7][8]. These methods focus on designing clean sheet aircraft and hence adapt the classical methods presented in texts such as Raymer[9] or Roskam[10]. As has been identified by many industry players, the initial stage will consider retrofits of previous aircraft as this involves less risk and capital expenditure. There are a few papers investigating performance and design of retrofitted aircraft; one paper [11] considered the design and performance of a small two seater aircraft retrofitted with a parallel hybrid electric propulsion system. Juretzko et al. analysed the retrofit of a 19-passenger aircraft with a series hybrid propulsion system [12].

Few studies have been conducted on comparing fully electric vs other potential technologies such as parallel or series hybrids and hydrogen propulsion. This study therefore aims at constructing a simple methodology to size retrofits using these different types of propulsion system architectures and compare their performance.

3. Methodology

This section presents the methods used in order to obtain the performance and cost estimates for a retrofitted aircraft. It begins by describing the main aircraft parameters required, followed by the sizing of the propulsion system. The mission performance analysis methods are then presented followed by the assumption used in the cost estimate.

3.1 Aircraft Parameters

In order to size the propulsion system a set of parameters need to be defined from the original aircraft. The first parameter is the maximum installed power of the engines P_{max}, for sake of simplicity, it will be assumed this power is equal to the maximum output power at the shaft of the propeller. The next parameters are the weights of the aircraft, in particular the sizing algorithm will need the following:

- Maximum Take-Off Weight (MTOW): Maximum allowed weight before take-off.
- Empty Weight (EW): Aircraft without fuel, pilots or payload.

For the purpose of retrofitting it is useful to define another weight which will be called the 'Baseline Empty Weight'(BEW). This weight is calculated by subtracting the major components related to the conventional internal combustion engine (ICE) system which is the fuel tank weight $W_{FuelTank}$ (also including the fuel system components) and the propulsion related weights $W_{Propulsion}$ of the original aircraft from the EW as seen in Equation (1).

$$W_{BEW} = W_{EW} - W_{Propulsion} - W_{FuelTank} \tag{1}$$

Finally, to be able to size the aircraft, knowledge of the aerodynamic drag is required. The simplified drag model is used [13] as shown in Equation (2).

$$C_D = C_{D_0} + \frac{C_L^2}{\pi ARe} \tag{2}$$

The parameters of C_{D_0} and e must be estimated. Performance and propulsion parameters required to size the aircraft will be discussed in section 3.3

3.2 Propulsion System Sizing

Since the strategy is to retrofit the aircraft, the method to size the different propulsion systems can use the existing power of the aircraft as the total shaft output power and the MTOW of the aircraft minus the payload can give a limit to the size of the battery system installed. This is done so that the maximum number of passengers the retrofit can carry is the same as in the original aircraft. These two principles of sizing, i.e power equivalence and weight restriction, are applied to the four architectures, each with its different efficiencies to take into account in order to obtain the final shaft output power. The different architectures considered are shown in figure 1.
The first sizing step is that of determining the power of each component. It is important to follow a consistent definition of what is meant by power, as this may or may not take into account the efficiency.

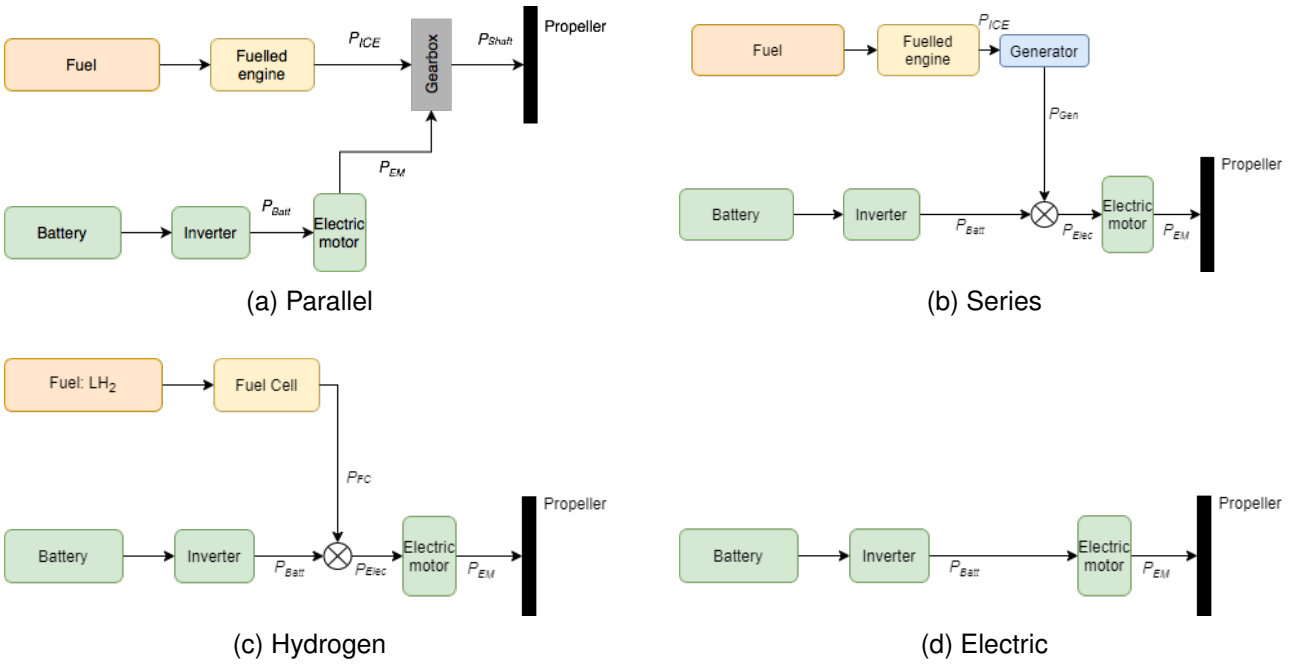

(a) Parallel (b) Series

(c) Hydrogen (d) Electric

Figure 1 – Propulsion architecture diagrams.

As stated in [14], the power is the installed power at the shaft of the component. From this the shaft power P can be formulated for each of the retrofits as shown in Equations (3)-(6).

$$Parallel: \quad P = (P_{ICE} + P_{EM}) \cdot \eta_{GB} \tag{3}$$

$$Series: \quad P = (P_{GEN} + P_{BAT}) \cdot \eta_{EM} = P_{EM} \tag{4}$$

$$Hydrogen: P = (P_{FC} + P_{BAT}) \cdot \eta_{EM} = P_{EM} \tag{5}$$

$$Electric: \quad P = P_{BAT} \cdot \eta_{EM} = P_{EM} \tag{6}$$

In the case of parallel, series and hydrogen fuel cell hybrids, it is required to prescribe the power split between electric and fuel consuming power plants; this is done by using the hybridization of power ratio, H_P. Its definition varies slightly depending on the retrofit however in general it is given by Equation (7).

$$H_P = P_{Elec}/(P_{Fuel} + P_{Elec}) \tag{7}$$

Where P_{Elec} describes the maximum electric energy coming from the electric motors in the case of the parallel architecture or the battery in the case of the series and hydrogen retrofits. The general fuel consuming maximum installed power is denoted by P_{Fuel}, where for the parallel this would be equal to the ICE installed power and for the series and hydrogen would be the generator and fuel cell powers respectively. As will be explained in the case study, the cruise segment is where most of the energy of the aircraft is spent. Since the energy per unit weight is higher for fuels compared to the battery, the power ratio will be such to allow the fuelled component of the propulsive system to sustain cruise conditions. This allows the hybridization ratio to be found using Equation (8).

$$H_P = 1 - \frac{P_{Shaft_{Cruise}}}{P_{Installed}} \tag{8}$$

The cruise shaft power $P_{Shaft_{Cruise}}$ is found from Equation (31) given in section 3.3 $P_{Installed}$ is the original maximum power of the aircraft. It must be noted that in order to size the components of the different architectures, different efficiencies must be taken into account. This will be described in detail in the following sections after the energy storage general methodology is presented.

To size the energy storage unit (i.e the battery), the weights of the components are used. A restriction is imposed such that the MTOW of the retrofit remains the same as that of the original aircraft.

In addition, the payload weight is kept constant for all the retrofits. From this the maximum weight available for the energy storage system can be found using Equation (9).

$$W_{EnergyStorage} = W_{MTOW} - (W_{BEW} + W_{Crew} + ... \\ W_{Payload} + W_{Propulsion}) \tag{9}$$

Equation (9) can be used for all architectures as the energy storage weight can be composed of different types of systems such as conventional AVGAS or kerosene fuel, battery or hydrogen systems. This weight should include the weight corresponding to the storage material too as well as the fuel stored in it. In this study the storage weight is assumed to be composed of a battery, a fuel tank and the fuel inside it as seen in Equation (10).

$$W_{EnergyStorage} = W_{Batt} + W_{FuelTank} + W_{Fuel} \tag{10}$$

The energy storage value can be obtained from Equation (9) as all terms on the right hand side are prescribed. In the case of parallel, series and hydrogen fuel cell retrofits, it is required to find W_{Batt} and W_{Fuel}. $W_{FuelTank}$ can be either assumed constant or can be given as a function of W_{Fuel} as will be the case for the hydrogen retrofit. This will be covered in section 3.2.3Hence in order to solve for the two unknowns a second equation is required. This equation comes from prescribing a hybridisation of energy ratio H_E defined in Equation (11). Now the fuel energy can be given in terms of the battery energy as shown in Equation (12).

$$H_E = \frac{E_{Batt}}{E_{Batt} + E_{Fuel}} \tag{11}$$

$$E_{Fuel} = \left(\frac{1}{H_E} - 1\right) E_{Batt} \tag{12}$$

Where E_{Batt} and E_{Fuel} are the energy content of the battery and fuel respectively. By relating the weights to the energy content via specific energies denoted by σ, the weight of the battery and fuel can be cast in terms of their energy content as shown in Equations (13) and (14).

$$W_{Batt} = E_{Batt}/\sigma_{Batt} \tag{13}$$

$$W_{Fuel} = E_{Fuel}/\sigma_{Fuel} \tag{14}$$

Substituting Equations (13) and (14) into (10) yields Equation (15). Finally substituting for the fuel energy in terms of the battery energy means the battery energy can be solved for as shown in Equation (16) and hence the storage system is sized.

$$\frac{E_{Batt}}{\sigma_{Batt}} + \frac{E_{Fuel}}{\sigma_{Fuel}} = W_{EnergyStorage} - W_{FuelTank} \tag{15}$$

$$E_{Batt} = \frac{W_{EnergyStorage} - W_{FuelTank}}{\left(\frac{1}{\sigma_{Batt}} + \frac{\frac{1}{H_E}-1}{\sigma_{Fuel}}\right)} \tag{16}$$

This sizing approach means the retrofit is not designed for a specific mission. The consequences are that range performance will be constrained by the sizing procedure. Therefore, when comparing the retrofits, a mission which all versions can meet will be used. This will be explained with a case study in section 4.

The next sections will detail specific procedures used for each of the retrofits in order to size the propulsion and energy storage system.

3.2.1 Parallel Hybrid

For the case of the parallel hybrid both the electric motor and the ICE engine provide power via some sort of mechanical link. In this report it will be assumed that the mechanical link will be a gearbox

with a certain specific weight which will be detailed in the case study. From this fact, the expression for power hybridisation can be formulated as shown in Equation (17).

$$H_P = \frac{P_{EM}}{P_{EM} + P_{ICE}} \Rightarrow P_{ICE} = P_{Shaft_{Cruise}} \tag{17}$$

Prescribing the ICE power installed to be equal to the cruise power required determines the amount of electric motor power since it needs to add up to the total installed power of the original aircraft. Since the electric motor is solely powered by the battery, prescribing a power of the electric motor will mean the battery will have a minimum size based on its maximum power. Nevertheless, the battery may be made larger to provide higher energy content. The relation between power and energy content of a battery depends on the specific architecture and layout of the battery. In this work, typical values of power density and energy density for batteries will be assumed.

3.2.2 Series Hybrid

The series hybrid produces all the propulsive shaft power using electric motors, hence a different variation of the power hybridisation ratio is used. For the series it is assumed that the fuel power comes from the generator, hence this must be sized to be able to sustain cruise. Equation (18) is used to obtain the size of the ICE component which is coupled to the generator. The maximum battery power output required can be calculated by Equation (19).

$$P_{ICE} = \frac{P_{Shaft_{Cruise}}}{\eta_{EM}\eta_{Gen}} \tag{18}$$

$$P_{Batt} = P_{Installed} - P_{ICE} \cdot \eta_{Gen} \tag{19}$$

Where η_{Gen} is the generator efficiency due to losses when the shaft power from the ICE is converted into electric power. It must be noted that this sizing approach does not consider one engine inoperative cases such as when the battery or ICE fails.

3.2.3 Hydrogen Fuel Cell

The hydrogen fuel cell architecture is very similar to the series with the difference being that the fuel cell replaces the ICE engine and electric generator. What follows is a brief description of how fuel cells operate. The proton exchange membrane (PEM) type is selected for the fuel cell as it has low startup times and adjusts quickly to power changes [15]. A fuel cell is composed of an electrolyte sandwiched between an anode and a cathode. At the anode, hydrogen is oxidised to produce hydrogen ions or protons which travel through the electrolyte. This produces electrons which can power an electric load. The hydrogen protons travel to the cathode where they react with oxygen to produce water. This reaction is exothermic and produces mild amounts of heat which requires a cooling system. The overall reaction is given here:

$$2H_{2_{(g)}} + O_{2_{(g)}} \rightarrow 2H_2O_{(l)} \tag{20}$$

The theoretical voltage of any single cell is 1.229V [16]. In order to achieve the power requirements of the aircraft, individual cells are stacked to form a 'fuel cell' stack. An important parameter is the current that is produced per unit area of cathode/anode plating. This 'current density' has several effects on the efficiency of the fuel cell stack. Without going into too much detail, these efficiencies can be quantified in terms of polarisation curves. This shows that as the power is increased towards the maximum, the fuel cell efficiency is decreased. This means that in order to obtain good efficiencies over-sizing the fuel cell is required. Nevertheless, a trade-off was found in [17] where, the actual effect of over sizing the fuel cell had to be coupled with a decrease in weight of the hydrogen required and hence tank weight. From this investigation, the fuel cell stack was sized using the required cruise power P_{Cruise}. It is then oversized by a factor ϕ of 1.33. This results in a fuel cell efficiency η_{FC} of 55%[17]. The polarisation curves from which this was obtained are included in Appendix B. From this the fuel cell installed power can be calculated using the cruise power requirement as shown in Equation (21).

$$P_{FC} = \frac{P_{Shaft_{Cruise}}}{\eta_{EM}\eta_{FC}} \cdot \phi \tag{21}$$

The hydrogen storage tank must be modelled as the weight will significantly vary depending on the volume of fuel carried. The method used assumes a number n of cylindrically shaped tanks with a certain area density ρ_{Tank} of the material in order to estimate the total weight as shown in Equation (22).

$$W_{Tank} = n \cdot A_{Tank} \cdot \rho_{Tank} \tag{22}$$

The surface area of single tank can be related to the volume of a single tank V_{Tank} via Equation (23). A slenderness ratio of the tank l is introduced: this is the length to diameter ratio. A value of $l = 4$ is fixed throughout this study.

$$A_{Tank} = l\pi \left(\frac{12}{\pi(3l-1)} \right)^{\frac{2}{3}} V_{Tank}^{\frac{2}{3}} \tag{23}$$

Assuming the volume of the tanks is equal to that of the fuel, the fuel energy can then be related to the volume and hence an expression for the weight of the tank in terms of fuel (or battery) energy can be obtained. This yields a non-linear equation (see Equation (24)) which can be solved numerically with schemes such as the Newton-Raphson method.

$$AE_{Batt} + BE_{Batt}^{\frac{2}{3}} = W_{EnergyStorage} \tag{24}$$

$$A = \frac{1}{\sigma_{Batt}} + \frac{1}{\sigma_{LH2}} \left(\frac{1}{H_E} - 1 \right) \tag{25}$$

$$\begin{aligned} B =& \rho_{Tank} n^{\frac{1}{3}} l\pi \left(\frac{12}{\pi(3l-1)} \right)^{\frac{2}{3}} \cdot \ldots \\ & \left(\frac{1}{\rho_{LH2}\sigma_{LH2}} \left(\frac{1}{H_E} - 1 \right) \right)^{\frac{2}{3}} \end{aligned} \tag{26}$$

For the derivations of the tank volume and area relations see Appendix A.

3.2.4 Fully Electric

The fully electric architecture is simpler to size since there is no split in power. Hence the electric motors are sized to output the same power as the original aircraft. Therefore the required battery output power is given by Equation (27).

$$P_{Batt} = \frac{P_{Installed}}{\eta_{EM}} \tag{27}$$

The battery is then sized according to the maximum allowable weight which can be added without impacting the payload. This results in a simplification of Equation (16) as no fuel is used. Hence Equation (28) can be used to find the battery energy available for the electric retrofit.

$$E_{Batt} = W_{EnergyStorage} \cdot \sigma_{Batt} \tag{28}$$

3.3 Mission Analysis

For the general aircraft, the fuel consumption and energy consumption is measured for 5 segments of the mission: 1) Taxi 2) Take-Off (TO), 3) Climb, 4) Cruise and 5) Descent & Landing. In addition, 3 more segments are added to the mission to account for reserve fuel, these are: 6) Reserve climb to 4000ft, 7) 45 minutes of loiter and 8) descent & landing. These segments are shown in figure 2.

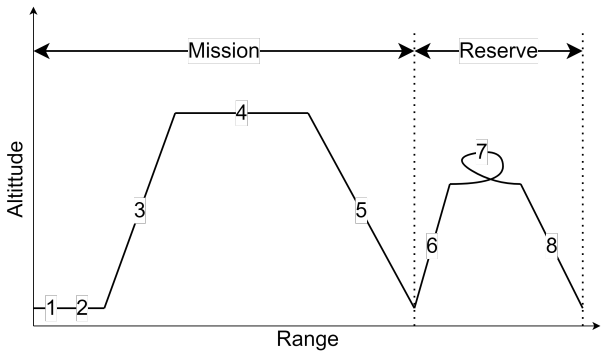

Figure 2 – Design mission profile.

Each segment has predefined performance parameters which are given as inputs as will be shown in the case study. Given this study is based on retrofitting existing aircraft, data from the Pilot Operating Handbook (POH) can be used to link power to performance. This is done for the TO and climb segments. The next section details how the energy consumption is calculated for a specific mission definition.

3.3.1 Taxi

The taxi out segment assumes a constant power which can be provided by either the electric motors or ICE engines. The energy can come form either a fuel or a battery. Except for the baseline configuration, battery power will be used for the entire duration of this phase to provide a quieter taxi which emits less pollution. Therefore the only inputs required for this segment are he time t_{Taxi} and the power P_{Taxi} setting which is assumed constant.

3.3.2 Take-Off

The TO segment energy consumption is computed in a similar fashion to the taxi. Nevertheless, instead of arbitrarily prescribing the time and power, these are actually sourced from the POH. For the power, the maximum installed power for all components is used. For the time, a constant acceleration is assumed, from which Equation 29 can be used.

$$a = \frac{V_{LoF}^2}{2s} \rightarrow t_{TO} = V_{LoF}/a \tag{29}$$

Where V_{LoF} is the lift off speed and s is the take-off distance. It must be noted that the take-off distance is usually defined as the horizontal distance required to reach 50ft, nevertheless the next climb phase is computed from 0ft. This inaccuracy is small and makes this method general and quick. A maximum error of 10% compared to methods from Gudmundsson [13] was found.

3.3.3 Climb

The climb is assumed to occur at the maximum Rate of Climb (RoC) quoted in the POH. This corresponds again to the maximum power setting for each of the components in the retrofit. The time is calculated assuming a constant RoC and is shown in Equation 30.

$$t_{Climb} = h_{cruise}/RoC_{max} \tag{30}$$

Where h_{Cruise} is the cruise altitude. This method is not accurate for very high h_{Cruise} as power loss due to altitude will reduce the RoC. This can be mitigated by selecting a RoC quoted for an altitude equal to $\frac{1}{2}h_{Cruise}$.

3.3.4 Cruise

The cruise segment is defined by either a time t_{Cruise} or a distance d_{Cruise}. Assuming no wind, these are linked via the cruise airspeed V_{Cruise}. The mission is discretised into various segments and the total instantaneous shaft power required is calculated using Equation (31).

$$P_{Shaft} = \frac{W}{L/D \cdot \eta_p} \cdot V_{Cruise} \tag{31}$$

Where W is the instantaneous weight at that point, L/D is the lift to drag ratio and η_p is the propulsive efficiency. Using the power split for the cruise segment, the amount of fuel or energy can be computed by multiplying the instantaneous power by the time step. This procedure allows the weight to vary for the cases where fuel is consumed.

3.3.5 Descent

The descent segment is defined by a descent rate RoD, a descent airspeed $V_{Descent}$ and the initial altitude which is equal to that of the previous cruise segment. The power required could be estimated using an analytic equation however it has been seen in other methods that a reasonable power to take during this segment is 15% of the maximum [6].

3.3.6 Reserve

The reserve segment assumes a climb back to a loiter altitude, which is in general different to the mission cruise altitude, followed by a 45 minute loiter and a descent back for landing. These three segments use the same approach as those described in the previous sections.

3.4 Powertrain modelling

In order to calculate the fuel and energy consumed by the different retrofits, a model must be used for the combustion engine, generator, fuel cell and battery.

3.4.1 Combustion Engine

Fuel used is typically calculated using a specific power fuel consumption denoted by C_{Power}. Hence from a required power by the internal combustion engine (ICE), the fuel consumed per unit time can be calculated using Equation (32). For each segment of the mission, the fuel consumed is subtracted from the weight of the aircraft using Equation (33), where the subscript i denotes a particular mission segment. the average consumption rate $\dot{W}_{fuel}$ is multiplied by the time of each segment as shown in Equation 33.

$$\dot{W}_{fuel} = P_{ICE} \cdot C_{Power} \tag{32}$$

$$W_{fuel_i} = \dot{W}_{fuel_i} \cdot t_i \tag{33}$$

3.4.2 Generator

The generator used in the series architecture is modelled as an electric engine working in reverse, i.e converting mechanical power into electric power. Mechanical power is fed from an ICE via a shaft. Hence the combination of ICE + generator will produce an electric power which is calculated using Equation (34), where η_{Gen} is the generator efficiency.

$$P_{Gen} = P_{ICE} \cdot \eta_{Gen} \tag{34}$$

The fuel consumed can be calculated using the same methods of Equations (32) and (33).

3.4.3 Fuel Cell

The fuel cell in the hydrogen architecture acts in a similar way to the generator, only this time the fuel weight is not calculated using a specific power fuel consumption but rather using the specific energy of the fuel σ_{LH2} and an efficiency η_{FC} as is described in section 3.2.3The fuel consumed can then be calculated using Equation (35).

$$\dot{W}_{fuel_{LH2}} = P_{FC} / (\sigma_{LH2} \cdot \eta_{FC}) \tag{35}$$

3.4.4 Electric Motor

The power output from the electric motor is modelled using a constant motor efficiency denoted by η_{EM}. It is important to define a nomenclature for powers as stated in Equations (3)-(6). The output shaft power is denoted by subscripts EM while the input by $Elec$. The input power P_{Elec} can come from various sources such as a generator, fuel cell or battery. Then the output power is calculated using Equation (36)

$$P_{EM} = P_{Elec} / \eta_{EM} \tag{36}$$

3.4.5 Battery

The energy and power output of a battery must be modelled. In the nomenclature used in this report, the battery power output is denoted by subscript $Batt$. This power is assumed to be fed directly into the electric motor and no loss due to the inverter is included in this part. The energy consumed from the battery does however account for inefficiencies such as cabling and an inverter. A simple model is used whereby a single efficiency is used to convert the power drawn from the battery by the electric motor into the energy consumed from the battery. This is shown in Equation (37) for the i^{th} segment, where η_{Batt} is the battery efficiency which accounts for losses due to cabling and the presence of an inverter.

$$E_{Batt_i} = P_{Batt_i} \cdot t_i / \eta_{Batt} \tag{37}$$

More detailed methods of analysing the battery can be used but for this high-level study, this method was found sufficient.

4. Case Study

The methodology described to size and analyse the retrofits is now applied to an actual aircraft to obtain a comparison of the costs required to fly each of the retrofits. Various aircraft can be chosen in the regional air mobility sector. Focusing on Part 23 aircraft, there are up to 19 passenger aircraft such as the Dornier-228 or DHC-6 Twin Otter. Fewer passenger models such as the Britten Norman Islander and the Tecnam P2012 are also options. The 7 passenger Piper PA31 Navajo shown in figure 3 was chosen for the case study.
Important data from the aircraft which is used during the analysis is presented in table 1[18].

Table 1 – Aircraft parameters obtained from [18]

Parameter	Value	Units
MTOW	2948	kg
EW	1815	kg
BEW	1249	kg
Wing Area	21.3	
AR	7.2	-
pax.	7	-
C_{D_0}	0.027	-
k	0.0551	-

The way the aerodynamic parameters C_{D_0} and k have been computed is given in Appendix C.

4.1 Mission Definition

Before sizing the retrofits, it is useful to understand the mission this aircraft will be used for. The mission is based on a typical island hopping commuter service, hence the cruise is relatively short. The altitude, speed and vertical velocities at each segment of the flight is given in table 2.

Table 2 – Mission definition and parameters.

Segment	Time (min)	Distance (km)	Altitude (ft)	Velocity (kts)	RoC (fpm)
Taxi	5.0	0.0	0	0	0
TakeOff	0.6	0.0	0	Accelerating	0
Climb	3.8	9.9	Climbing	84	1300
Cruise	15.0	71.3	5000	154	0
Descent	7.1	30.8	Descending	140	-700
Reserve	49.4	215.3	2000	130	0

The shaft power required at each segment can be estimated since it is almost independent of the retrofit. In reality, the cruise segment power depends on the weight of the aircraft which is determined by the fuel consumed and therefore varies slightly from one retrofit to another. Nevertheless, the assumption of equal shaft power across all retrofits is useful information for sizing. In figure 4, the energy split is shown for each of the main mission segments. The reserve is not included.

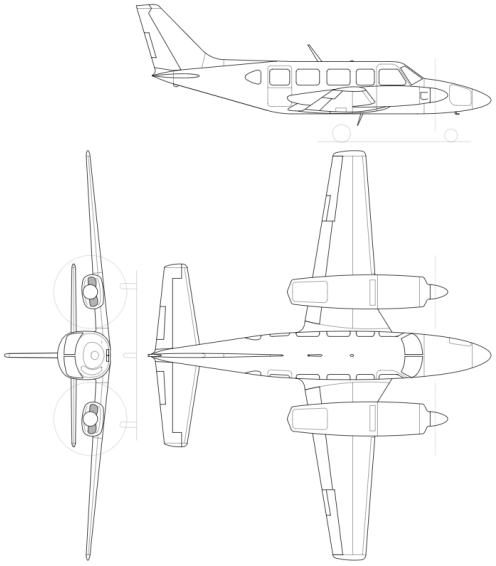

Figure 3 – Piper Navajo schematic drawing[19].

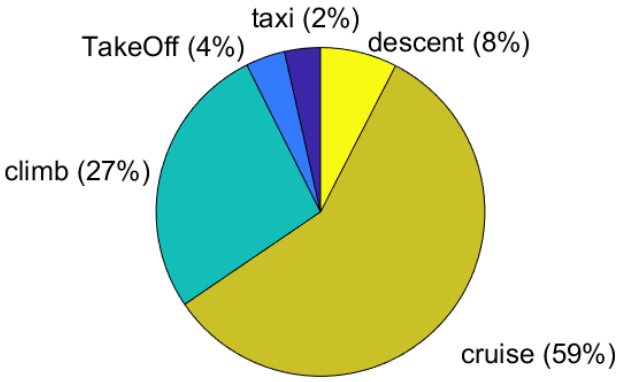

Figure 4 – Energy distribution for the design mission.

4.2 Retrofit Sizing

The different retrofits can now be sized using the methodology laid out in section 3.2 In order to be able to compare the retrofits in a reasonably similar manner, the internal combustion technology will be kept the same for the parallel and series hybrids. As mentioned in section 3.the sizing is determined by a power matching, weight constraint and the prescription of the hybridisation ratios H_P and H_E for power and energy respectively. To determine a suitable hybridisation of power, information from the mission is used. As seen before, the cruise segment is where most of the energy is spent. Since it is known that fuel (both petrol and hydrogen) have a much better specific energy density than batteries do, the fueled component of the propulsion architecture will be sized so that it can at least produce the power required for cruise.

In the case of the parallel architecture, the power deficit at take-off and climb will be solved by adding electric engines. On the other hand, series and hydrogen fuel cell architectures have their deficit covered by electric energy coming from the battery instead of the generator or fuel cell.

As an example, the parallel architecture is considered. From the required cruise power the hybridisation of power for the parallel architecture can be calculated as shown in Equation (39).

$$P_{ICE} = P_{Cruise} = 253\text{kW} \tag{38}$$

$$H_p = \frac{P_{EM}}{P_{Total}} = 1 - \frac{P_{ICE}}{P_{Total}} \approx 0.45 \tag{39}$$

The next parameter which defines the retrofit is the hybridisation of energy H_E. In general these values are low since the batteries are heavy and having a lot of energy stored as electrical energy would mean there is little weight for fuel which is what actually gives the retrofit a decent range. It is decided to keep H_E equal between all retrofits in order to do as fair of a comparison as possible. The main constraining retrofit was the series architecture due to its large weight of the propulsion

system leaving very little left for the energy storage. Hence while a hybridisation ratio of 20% can be used in the parallel architecture, the series would not have enough fuel at maximum payload to perform the targeted mission. A final value of $H_E = 5\%$ is used as this provided a reasonable sizing for all the retrofits. A payload-range plot (see figure 5) was used to evaluate the resulting retrofits, although this is not critical for aircraft designed for short hops, the flexibility might indeed be useful.

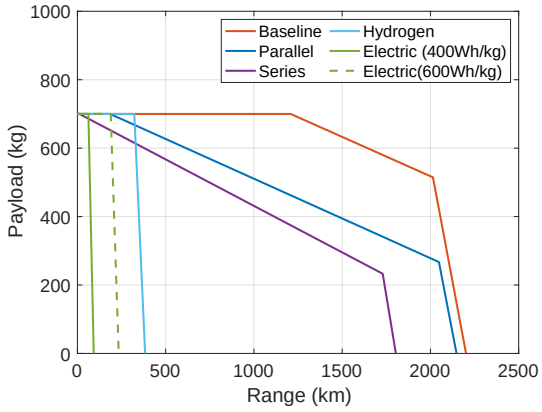

Figure 5 – Payload vs range for the different architectures.

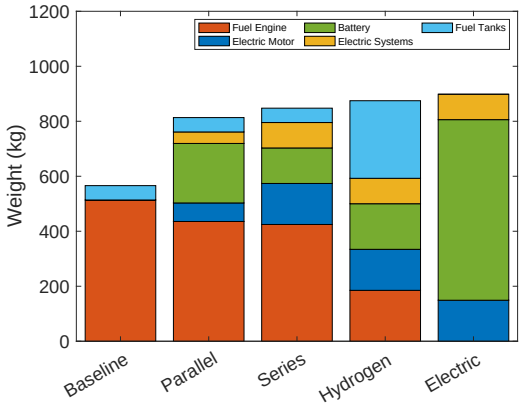

Figure 6 – Weight analysis of the resulting propulsion system retrofits.

There are some important points to mention from the payload range diagram. Firstly, both the parallel and series have very little decrease in maximum range. The hydrogen retrofit seems to preform quite poorly in terms of maximum range. This is due to the limited volume external storage tanks can have without drastically increasing drag and weight. The hydrogen retrofit does however have better range than any of the retrofits at full payload and the series struggles the most. Finally mention that the fully electric retrofit can only perform the mission if the battery specific energy is higher than 320Wh/kg. A reasonable value to use currently is 250Wh/kg [20] and is the value that is used for all other retrofits.

4.3 Summary of Sizing results

The installed powers of the fuelled component and the electric motors are shown in table 3.

Table 3 – Summary of powertrain and energy storage data.

Retrofit	Power (kW)		Energy (kWh)	
	Fuel	Elec	Fuel	Batt
Baseline	462	0	4022	0
Parallel	253	209	1028	54
Series	296	462	613	32
Hydrogen	338	462	844	44
Electric(400Wh/kg)	0	462	0	263

4.4 Weight analysis

With the sized components, the weight of the propulsion system can be obtained. In order to do so, certain power and energy densities were used for the electric motor, battery, ICE engine, fuel cell and hydrogen tank. These values may change as technology improves. The values used are given in table 4. The weights of the resulting propulsion system and energy storage is shown in figure 6. Note that fuel is not included here however it can be assumed that the fuel carried by each of the retrofits, at maximum payload capacity, will make the bars extend to the limit of the electric retrofit. The raw data is given in Appendix D. It must be noted that in the case of the series and hydrogen retrofit, the fuel engine are the ICE+generator and the fuel cell respectively. Quite counter intuitively,

Table 4 – Power and energy densities used to compute the weights.*Note the electric retrofit used 0.4kWh/kg and 0.6kWh/kg as battery energy densities.

Component	Value	Units
Electric Motor	3.1	kW/kg
Battery*	0.25	kWh/kg
ICE	0.9	kW/kg
Gearbox	3.0	kW/kg
Fuel Cell	1.6	kW/kg
Electric Systems	5.0	kW/kg
LH2 Fuel Tank	75.0	$\mathrm{kg/m^2}$

Table 5 – Specific Energy of fuels used in the retrofits.

Fuel	AVGAS	LH2
Energy Density kWh/kg	12.1	33.3
Vol. Energy Density $\mathrm{kWh/m^3}$	8712.0	2359.3

the fuel engine weight of the parallel is similar to the series architecture, but the series has a higher installed power. This is due to the fact the parallel has an installed gearbox which weighs 150kg.

4.5 Mission Analysis

The sized retrofits can now be analysed on the same mission to compare their energy usage and the cost derived from these. Before presenting the results for energy consumption, a few parameters need defining in order to be able to calculate the fuel consumed. First of all the specific energy content of each fuel is given in table 5. This is required in order to convert a weight of fuel used into energy used. The mass specific energy density of the pressurised liquid hydrogen is better than the carbon based fuel. Nevertheless, the catch is in the volume, where hydrogen requires roughly 4 times as much to store the same amount of energy.

The fuel consumption of the ICE engines used for the retrofits is taken from the baseline engine to be $0.27\mathrm{kg/kWh}$. The fuel cell fuel consumption is calculated using the energy density of the fuel and an efficiency. The efficiency of the components is given in table 6.

Table 6 – Efficiencies used for each of the components.

Component	Electric Motor	Battery	Generator	Fuel Cell
Efficiency	0.95	0.9	0.9	0.55

To compare the performance, the total energy consumed for the mission is computed and shown in figure 7. The raw data containing power, fuel and battery energy consumption is given in Appendix E. A measure of efficiency can be obtained by comparing the total energy spent from either fuel or battery sources to a theoretical value. This theoretical value is obtained by assuming 100% efficiency and is shown in grey in figure 7. These values are shown in table 7.

Table 7 – Energy efficiencies for each of the retrofits during the whole mission.

Retrofit	Efficiency
Baseline	28.2
Parallel	30.9
Series	28.8
Hydrogen	61.0
Electric	86.4

Furthermore, the reduction in fuel consumed by the parallel and serial hybrid compared to the baseline can also be obtained as shown in table 8. As was expected by [6], the series performs slightly worse on this metric.

Table 8 – Fuel consumption comparison of parallel and series against baseline.

Retrofit	Baseline	Parallel	Series
Fuel (l)	44.4	35.5	40.8
Decrease (%)	0	20	8

4.6 Cost Analysis

The costs per unit energy used are shown in table 9.

Table 9 – Energy source costs.

Source	AVGAS	LH2 Grey	Electricity
Cost (US Cents/kWh)	31.3	50.0	10.4

The costs are shown in figure 8 where the contribution from avgas fuel, electric energy and hydrogen fuel can be seen.

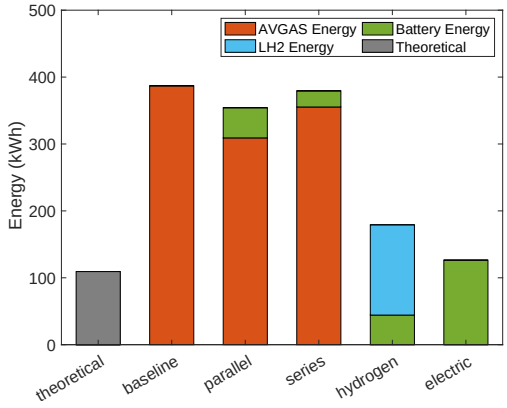

Figure 7 – Energy consumption of all the retrofits.

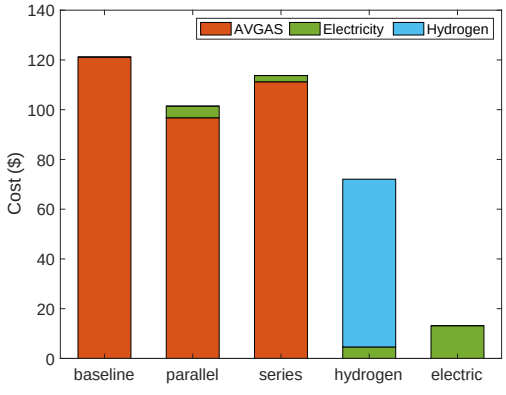

Figure 8 – Total costs of the retrofits.

The costs per available seat mile (note miles are statue) are given in table 10. The electric retrofit was ignored from this table as the battery technology used to obtain these results is 4 times better than what the rest of the retrofits used. The raw data of these costs is given in Appendix F.

Table 10 – CASM for all the retrofits except the electric.

Retrofit	Baseline	Parallel	Series	Hydrogen
CASM	24.9	20.8	23.3	14.8
Diff. (%)	0	16	6	41

5. Conclusion

From this study it has been shown that a simplified general sizing procedure can be used to size retrofits of the parallel, series, hydrogen fuel cell and fully electric kind. The restrictions imposed on weight are most constraining on the series which requires the electric motors to be sized to produce the total installed power while the parallel architecture can benefit from a lower electric engine weight. This weight restriction means that at full payload the series architecture would only be able to cover 11.2km (6.1nm). The hydrogen fuel cell has the largest range at full payload but the restriction imposed on the weight and the fact only two hydrogen tanks carried beneath the wing are used limits the maximum amount of hydrogen significantly and hence the range. From the mission analysis, the parallel architecture performed better than the series as was expected. Excluding the electric retrofit, the hydrogen had the best overall efficiency and hence operating cost values. With this study, it is seen that electrification of aircraft indeed improves the operational cost while full electrification on retrofits is still too constrained by the battery energy density to have any meaningful operational mission. All the results are available from the source code at `https://github.com/Pablodefelipe/economics_sustainable_aviation`.

6. Further work

It is clear that the simple sizing method does not provide an optimum performance as described in the literature [20]. Even with retrofits, the installed power can be increased, allowing for an increase in MTOW and providing better range or higher electrification which would reduce the costs. This is the strategy employed by the Rolls Royce- Tecnam PVolt retrofit. Using this framework could study the optimum Hp and He by letting MTOW be free. Another interesting concept is how the novel propulsion systems can produce aerodynamic and structural benefits when integrated into the airframe. As an example, the series architecture could allow for distributed propulsion architectures and boundary layer ingestion technology which could reduce the wing size or drag. Furthermore the addition of hydrogen tanks as under-slung pods will create extra drag which this analysis has neglected for ease of comparison.

7. Acknowledgements

The author wishes to thank the Ampaire UK team. Without their collaboration and insights, this report could not have been produced. A much deserved recognition for this research opportunity is directed to Dr. Daqing Yang. Finally, this report was written as an Undergraduate Research Opportunity within the department of Aeronautics at Imperial College London.

8. Contact Author Email Address

mailto: pablodfs123@gmail.com

9. Copyright Statement

References

[1] Moore MD. The third wave of aeronautics: On-demand mobility. SAE Transactions. 2006:713-22.

[2] Kreimeier M, Stumpf E, Gottschalk D. Economical assessment of air mobility on demand concepts with focus on Germany. In: 16th AIAA Aviation Technology, Integration, and Operations Conference; 2016. p. 3304.

[3] Schäfer AW, Barrett SR, Doyme K, Dray LM, Gnadt AR, Self R, et al. Technological, economic and environmental prospects of all-electric aircraft. Nature Energy. 2019;4(2):160-6.

[4] Ploetner KO. Operating cost estimation for electric-powered transport aircraft. In: 2013 Aviation Technology, Integration, and Operations Conference; 2013. p. 4281.

[5] Moore MD. Misconceptions of electric aircraft and their emerging aviation markets. In: 52nd Aerospace Sciences Meeting; 2014. p. 0535.

[6] Finger DF, Braun C, Bil C. An initial sizing methodology for hybrid-electric light aircraft. In: 2018 Aviation Technology, Integration, and Operations Conference; 2018. p. 4229.

[7] Pornet C. Conceptual design methods for sizing and performance of hybrid-electric transport aircraft. Technische Universität München; 2018.

[8] Elmousadik S, Ridard V, Secrieru N, Joksimovic A, Maury C, Carbonneau X. New Preliminary Sizing Methodology for a Commuter Airplane with Hybrid-Electric Distributed Propulsion. In: Advanced Aircraft Efficiency in a Global Air Transport System (AEGATS 18); 2018. p. 1-11.

[9] Raymer D. Aircraft design: a conceptual approach. American Institute of Aeronautics and Astronautics, Inc.; 2012.

[10] Roskam J. Airplane design part I. Preliminary sizing of airplanes. 1985;1.

[11] Xie Y, Savvaris A, Tsourdos A. Sizing of hybrid electric propulsion system for retrofitting a mid-scale aircraft using non-dominated sorting genetic algorithm. Aerospace Science and Technology. 2018;82:323-33.

[12] Juretzko P, Immer M, Wildi J. Performance analysis of a hybrid-electric retrofit of a RUAG Dornier Do 228NG. CEAS Aeronautical Journal. 2020;11(1):263-75.

[13] Gudmundsson S. General aviation aircraft design: Applied Methods and Procedures. Butterworth-Heinemann; 2013.

[14] Guidelines for Analysis of Hybrid Electric Aircraft System Studies. AIAA; 2019.

[15] Arangth Josef O. Conceptual Study of a Hybrid-Electric Airliner Using Hydrogen Fuel Cells. Final Year Project. 2021.

[16] Spiegel C. PEM fuel cell modeling and simulation using MATLAB. Elsevier; 2011.

[17] Kadyk T, Winnefeld C, Hanke-Rauschenbach R, Krewer U. Analysis and design of fuel cell systems for aviation. Energies. 2018;11(2):375.

[18] Piper. Piper PA-31 Navajo Pilot Operating Handbook; 1979.

[19] Wikipedia, the free encyclopedia. Piper PA31 three view drawing;. [Online; accessed December 4, 2021]. Available from: `https://commons.wikimedia.org/wiki/File:PiperNavajo.svg`.

[20] Finger DF, Braun C, Bil C. Case studies in initial sizing for hybrid-electric general aviation aircraft. In: 2018 AIAA/IEEE Electric Aircraft Technologies Symposium (EATS). IEEE; 2018. p. 1-22.

A Hydrogen Tank

The hydrogen tank is modelled as a cylinder where the total volume is given in Equation (40). A slenderness ratio parameter is used: $l = L/D$ where L is the length and D the diameter of the tank.

$$V_{Tank} = \frac{4}{3}\pi\left(\frac{D}{2}\right)^3 + \frac{\pi D^2}{4}(L-D) \qquad (40) \qquad V_{Tank} = \frac{1}{12}\pi D^3(3l-1) \qquad (41)$$

The surface area of a single tank A_{Tank} is given by Equation 42 and a compact form is given in Equation 43 when the slenderness ratio is used as a parameter.

$$A_{Tank} = \pi D^2 + \pi D(L-D) \qquad (42) \qquad A_{Tank} = l\pi D^2 \qquad (43)$$

B Fuel Cell polarisation curves

The polarisation curves for a typical fuel cell are given in figure 9[17].Figure 10 shows how the efficiency changes with the percentage of throttle, this is used to oversize the fuel cell.

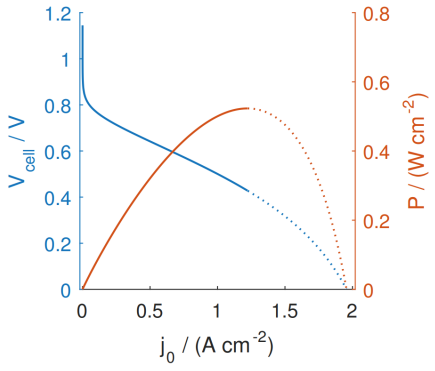

Figure 9 – Polarisation curves from [17].

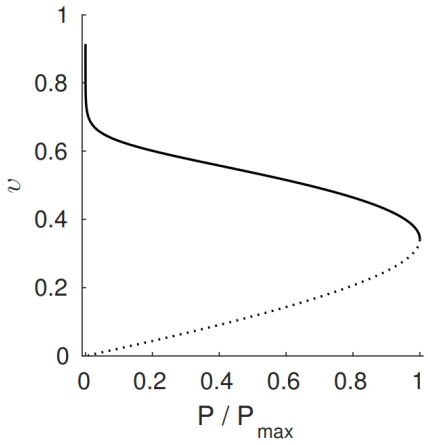

Figure 10 – Efficiency curves obtained from [17].

C Aerodynamic parameters

The zero lift drag was derived from cruise data quoted in the pilot operating handbook [18]. The raw and computed data is displayed in table 11.

Table 11 – Zero lift drag calculations

TAS (KIAS)	Power (BHP)	TAS (m/s)	Power (kW)	Thrust (N)	C_L	C_D	C_{D_i}	C_{D_0}
172	460	88.5	343	3101	0.283	0.0304	0.0044	0.0260
161	400	82.8	298	2881	0.323	0.0322	0.0058	0.0265
148	340	76.1	254	2664	0.383	0.0352	0.0081	0.0272

An average is taken from the computed values in table 11. The value of k is calculated assuming an Oswald efficiency of 0.8.

D Weight data

Table 12 – Weight analysis raw data in kg.

Mass (kg)	Baseline	Parallel	Series	Hydrogen	Electric
Mass	Baseline	Parallel	Series	Hydrogen	Electric
fuel engine	513.7	435.5	424.7	185.1	0.0
electric Motor	0.0	67.4	149.1	149.1	149.1
Battery	0.0	216.4	129.2	165.8	656.8
Elec. systems	0.0	41.8	92.5	92.5	92.5
Fuel Tank	52.2	52.2	52.2	282.2	0.0

E Mission Performance raw data

5.1 Baseline

Table 13 – Baseline raw data.

Segment	Taxi	TakeOff	Climb	Cruise	Descent	Reserve
Avg.Power(kW)	0.0	462.3	462.3	252.5	69.4	189.7
Fuel (USgal)	0.5	0.5	3.7	6.3	0.8	16.1

5.2 Parallel

Table 14 – Parallel raw data.

Segment	Taxi	TakeOff	Climb	Cruise	Descent	Reserve
Avg.Power(kW)	0.0	253.3	253.3	175.1	69.4	183.6
Fuel (USgal)	0.0	0.3	2.0	6.3	0.8	15.5
Elec.Power(kW)	46.2	209.1	209.1	77.6	0.0	6.5
ElecEnergy(kWh)	4.5	2.2	15.7	22.7	0.0	6.3
Batt.State(kWh)	54.1	49.6	47.4	31.7	9.0	9.0

5.3 Series

Table 15 – Series raw data.

Segment	Taxi	TakeOff	Climb	Cruise	Descent	Reserve
Avg.E.Power(kW)	46.2	462.3	462.3	252.7	69.4	189.9
ICE. Power(kWh)	0.0	296.2	296.2	288.1	81.1	214.5
Fuel (USgal)	0.0	0.3	2.3	7.1	1.0	18.1
Gen.Energy(kWh)	0.0	2.4	17.1	64.8	8.7	175.8
BattEnergy(kWh)	4.5	2.2	15.7	1.7	0.0	6.3
Batt.State(kWh)	32.3	27.8	25.5	9.9	8.2	8.2

5.4 Hydrogen

Table 16 – Hydrogen raw data.

Segment	Taxi	TakeOff	Climb	Cruise	Descent	Reserve
Avg.E.Power(kW)	46.2	462.3	462.3	253.2	69.4	195.1
FC. Power(kW)	0.0	253.3	253.3	188.3	73.0	198.1
Batt.Power(kW)	48.7	233.4	233.4	74.3	0.0	0.0
Fuel (USgal)	0.0	0.5	3.3	9.6	1.8	33.2
BattEnergy(kWh)	4.5	2.4	16.6	20.6	0.0	6.6
Batt.State(kWh)	54.1	49.6	47.2	30.6	10.0	10.0

5.5 Electric

Table 17 – Electric raw data.

Segment	Taxi	TakeOff	Climb	Cruise	Descent	Reserve
Avg.E.Power(kW)	46.2	462.3	462.3	253.3	69.4	191.3
BattEnergy(kWh)	4.5	5.0	34.7	74.1	8.3	13.9
Batt.State(kWh)	262.7	258.2	253.2	218.6	144.5	136.3

F Cost data

Table 18 – Raw data for the costs of the retrofits

Retrofit	Baseline	Parallel	Series	Hydrogen	Electric
Fuel ($)	121.1	96.8	111.2	67.4	0.0
Elec. ($)	0.0	4.7	2.5	4.6	13.1
Total ($)	121.1	101.4	113.7	72.1	13.1